ELSEVIER

Wear 209 (1997) 84–95

WEAR

# Experimental measurement of the residual stress field within thermally sprayed rolling elements

R. Ahmed *, M. Hadfield

*Brunel University, Department of Mechanical Engineering, Uxbridge, Middlesex UB8 3PH, UK*

Received 27 June 1996; accepted 7 January 1997

**Abstract**

A non-destructive experimental approach using an X-ray diffraction technique was used to investigate the generation of residual stresses in thermally sprayed rolling elements. The rolling elements were detonation gun coated balls and high velocity oxy-fuel coated cones. A modified four ball machine was used to perform rolling contact fatigue (RCF) tests on tungsten carbide cobalt (WC–Co) coated samples on steel substrate. RCF tests were conducted in conventional steel ball bearing and hybrid ceramic configurations. Residual stress measurements were performed at different sample orientations on different coating thicknesses and various substrate geometries. Residual stress measurements on as-sprayed samples, pre-tested samples, and after the RCF tests were performed during this study. This enabled the measurement of residual stresses generated during the thermal spraying process and due to the RCF tests. Residual stress measurements are also made on the failed areas of the coatings.

Residual stress measurement results are presented in the form of principal stress values, using complex stress/strain relationships. These results indicate that residual stresses are critical to the performance of coatings. The generation of residual stresses is not only dependent upon the coating process but also on the coating thickness and substrate geometry. RCF tests induce tensile residual stresses within the contact area and coating microstructure. Residual stress magnitude depends upon the test configuration and time of failure. Compressive residual stresses caused by the coating process are helpful as they improve the RCF life of the coatings. A multiple-cause diagram relating to the generation of residual stresses within the coatings has been presented and stress measurements have been explained with the aid of figures and scanning electron microscopy observations. © 1997 Elsevier Science S.A.

*Keywords:* Residual stress; Rolling contact fatigue; Thermal spray coatings

## 1. Introduction

### *1.1. Introduction*

The specific nature of the thermal spraying process results in the generation of residual stresses within the coating microstructure. The magnitude and direction of these stresses depends upon the nature of the coating process and the parameters controlled during the coating process. The magnitude of these residual stresses values can range up to hundreds of mega-Pascals (MPa). They can be critical to the performance of these coatings, where they are used for engineering applications involving mechanical or thermal loading. This study considers one such application in which these coatings are considered for improving the fatigue life of the inner and the outer race in rolling element bearing. Previous studies on the surface and subsurface residual stress fields in conventional steel ball bearing have shown that compressive residual stresses can significantly improve the bearing life [1]. Moreover, the studies by Bush et al. [2], Zaretsky et al. [3], Pomeroy et al. [4], Muro et al. [5] and Chen et al. [6] indicate that the generation of residual stress in rolling contact can be critical to the rolling contact fatigue (RCF) performance and the stress field depends upon the tribological conditions. These studies indicate that maximum compressive residual stress can occur at the location of maximum orthogonal shear stress, maximum shear stress or on the surface. The residual stress investigations can thus provide an improved understanding of the rolling contact fatigue behaviour of thermal spray coatings. This experimental research addresses the nature and magnitude of surface residual stresses within tungsten carbide cobalt (WC–Co) coatings, which are developed not only during the coating process but also after these coatings have been subjected to RCF tests.

RCF tests are conducted on a modified four ball machine which simulates the configuration of a rolling element ball

* Corresponding author.


*PII* S0043-1648(97)00009-4

bearing. The experimental residual stress measurements are made using an X-ray diffraction technique, which is not only a non-destructive technique and gives accurate residual stress measurements, but is also capable of measuring within precise locations (0.3 $mm^2$). The residual stresses are measured within the as-sprayed, pre-test and post-test conditions. Rolling elements in the geometry of ball, and cone coated by detonation gun (D-Gun, SDG2040) and high velocity oxy-fuel (HVOF) processes respectively are investigated for RCF performance. These coated rolling elements are then analyzed by residual stress X-ray measurements before and after the RCF tests. Measurements are also made within failed areas of the tested samples and principal stresses using complex stress/strain relationships have been used to present the results.

### *1.2. The generation of residual stresses in thermal spray coatings*

The thermal spraying technique involves a process in which a stream of high speed particles, in a molten or semi-molten state, lands on an underlying lamella or substrate which is usually sand blasted. The nature of the coating process, thermal and mechanical properties of the substrate and the coating material, the preheat temperature of the substrate, and the particle speed are the major factors which effect the generation of the residual stress field (Fig. 1).

It has been established that during the thermal spraying process each molten- lamella lands on an already solidified lamella resulting in macro stresses of tensile nature commonly known as the quenching stress within the individual splats [7]. This is because of an inelastic behaviour of the deposited splat since its contraction is constrained by the underlying lamella. This also results in the generation of the micro stresses at the interface of the lamellas. Gill [8] described a variety of phenomena which explain the relaxation of these stresses by interfacial sliding, micro-cracking, etc. With the advancements of high velocity processes particle speeds up to 750 m $s^{-1}$ are achieved which cause a shot-peening effect on the underlying lamella and, as a result, macro stresses of compressive nature are generated in the coatings.

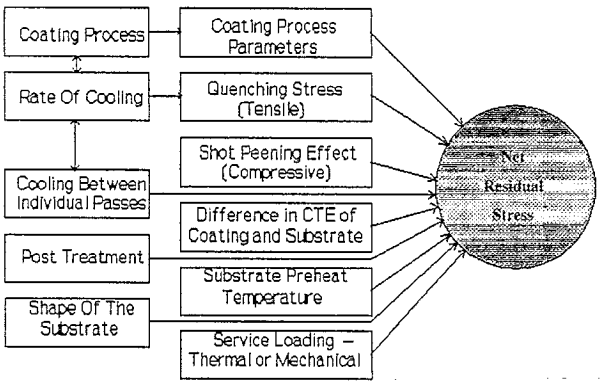


Fig. 1. Factors affecting the residual stress generation.

The rate at which these coatings cool, specially between the individual passes of spraying also affects the generation of these stresses. During the thermal spraying process the substrate temperature increases, whereas the temperature of the deposited lamellas decreases because of their heat conduction into the substrate, and heat convection and radiation into the immediate environment. After the thermal spraying process an equilibrium is reached when the coating bulk temperature equals the substrate temperature. Then the substrate and coating cool until the bulk temperature reaches the atmospheric equilibrium temperature. During this cooling process, both the coating and the substrate contract at a rate which depends upon their individual coefficient of thermal expansion. This difference in the coefficient of thermal expansion creates residual stresses of compressive or tensile nature in the coating and the substrate. Post treatment of the coating eg. heat treatment, hot isostatic pressing or grinding will also affect the residual stress field. Fig. 1 represents a multiple cause diagram of the factors which are important to the development of the micro- and macro-residual stresses field within thermal spray coatings. The overall stress value within a coating can vary significantly throughout the coating thickness, depending upon the combination of significant local factors at particular locations. The phenomenon is more complicated for substrate shapes of varying geometry, since the rate of heat transfer and the cooling intensity will vary. Moreover, the anisotropy of thermally sprayed coatings causes variations in the magnitude and orientation of these stresses, not only in the as-sprayed conditions but also during the service conditions involving mechanical or thermal loading. The case is worst for a cyclic loading process because individual passes of load can cause plastic deformation within the coating microstructure which result in the generation of residual stresses. The process of plastic deformation can continue until the shakedown limit is reached in the layered surface [9].

### *1.3. Previous experimental studies*

Previous studies related to the magnitude and orientation of residual stress induced in WC–Co coatings deposited by a variety of processes, ie. HVOF, air plasma spraying (APS), jet-kote (JGun) and continuous detonation spraying (CDS) etc., reveal different results.

Provot et al. [10], in their experimental study of residual stress in WC–Co coatings on a $Ti_6Al_4V$ substrate deposited by APS and CDS processes, reported a gradient of the residual stress magnitude throughout the coating thickness. These measurements were achieved by using a step-by-step hole drilling technique. These stresses were of tensile nature with the values much higher for APS coatings in comparison to the CDS coating method. A similar phenomenon was observed by Grevinge et al. [11], when they discovered that WC–Co coatings deposited by the HVOF process on a $Ti_6Al_4V$ substrate can induce residual stresses of tensile or

compressive nature or a combination of both within the coating thickness.

Knight et al. [12] in their study applied a different approach using an Almen test strip methodology for the measurement of the residual stress in WC–Co coatings deposited by JGun (JP5000). They reported significant changes in the stress values by varying the parameters controlled during the coating process. Morishita et al. [13], in their study of residual stress using the drilling technique, revealed that the stress induced by plasma spray WC–Co coatings on aluminium substrate are of tensile nature whereas JGun coatings produce compressive stress in these coatings. Similarly Brandt [14], during his study of residual stress in WC–Co coatings on an aluminium substrate, found that the magnitude of these stresses increases with an increase of the coating thickness.

In general it has been observed that the magnitude and orientation of these residual stresses depends not only upon the coating techniques and the parameters during the coating process, but also on the measurement method.

### *1.4. Experimental techniques of residual stress measurement*

#### *1.4.1. Review of experimental residual stress measurement*

There are many techniques available to measure the residual stresses in engineering materials. The anisotropy of thermally sprayed coatings [15] makes it difficult to provide a measurement of the stress distribution prevailing within the coating microstructure. X-ray diffraction is a non-destructive technique which can be employed to measure the residual stress field. This method can enable the measurement of the generation of these stresses not only due to thermal spraying process but also due to service loading. Bending tests for the measurement of these stresses give an overall value of macro stresses in a coating substrate combination, but tell little about the distribution of stresses within the coating. Moreover no information is provided about the micro stresses. The deep hole drilling technique is useful in determining the stress distribution in a coating but the process is destructive and assumes that the coating is homogeneous. These techniques require a knowledge of the values of physical properties like the Poisson's ratio and modulus of elasticity. Unfortunately, the values of modulus of elasticity and Poisson's ratio vary significantly for different coating processes and there is poor agreement between the values obtained from different measuring techniques [16]. Techniques like the Almen strip method [12] need to be fully developed before any meaningful results can be obtained. Computer models using numerical treatment can be helpful but need to consider a variety of factors some of which are shown in Fig. 1. This makes the problem complex and expensive to solve.

New approaches are required to measure these stresses to provide a detailed analysis of the stress distribution within the coating. As the residual stress varies at different orientations owing to the anisotropy of the coatings, stress measurement results can be presented in terms of principal stresses using a strain gauge analogy and complex stress/strain analysis in the X-ray diffraction technique.

#### *1.4.2. X-ray diffraction technique of residual stress measurement*

The X-ray diffraction technique has the capacity to accurately measure the magnitude and orientation of both macro- and micro-residual stresses by non-destructive analysis. These features can enable the investigation of the generation of residual stress due to the coating process and the RCF tests. This technique measures a change of a diffraction peak caused by the change in lattice spacing. A knowledge of the elasticity modulus ($E$) and Poisson's ratio ($\nu$) can enable the measurement of residual stress. The $\sin^2\psi$ technique of X-ray diffraction is used for residual stress measurements. Residual strain is calculated using the Bragg's equation:

$$n\lambda = 2d \sin\theta$$

$$\epsilon = \frac{\Delta d}{d} = \cot\theta_d \, \Delta\theta$$

where $n$ is the positive integral number indicating the order of diffraction, $\lambda$ is the X-ray wavelength, $d$ is the interplanar spacing in the crystal, $\theta$ is the diffraction angle, $\epsilon$ is the quantity of strains and, $\theta_d$ is the diffraction angle in a stress free condition. The stress ($\sigma$) on the surface is then calculated from the following expression:

$$\sigma = \frac{E}{1+\nu}\frac{\partial(\epsilon)}{\partial(\sin^2\psi)} = -\frac{E\cot\theta_d}{2(1+\nu)}\frac{\partial(\theta)}{\partial(\sin^2\psi)}$$

where $\psi$ is the angle between the sample normal and diffraction-plane normal. The above equation may be expressed as a product of constant $K$ and gradient $M$ using the equation:

$$\sigma = KM \tag{1}$$

where

$$K = -\frac{E\cot\theta_d}{2(1+\nu)}$$

and

$$M = \frac{\partial(\theta)}{\partial(\sin^2\psi)}$$

In Eq. (1) above, $K$ is an elastic constant for the X-ray stress measurement and $M$ is the gradient of the data regression line representing the stress results for various $\psi$ angles, typically from 0° to 40°. A more detailed description of residual stress measurement by X-ray diffraction can be found in Farrahi et al. [17]. The value of $K$ in the above equation was measured using a conventional in-situ four-point bending test equipment subjected to a known stress within the elastic range. The details of the method has been described by Cullity [18] and the measured value was $-466$ MPa deg$^{-1}$.

The penetration depth of X-rays for residual stress measurements varies for different sources of X-rays and the prop-

erties of material to be analyzed. Hadfield et al. [19] in their study of residual stresses described the penetration depths for different sources of X-rays. Most of the coatings suffer from the drawback of low penetration depths and hence require layer removal techniques like electrolytic polishing for the measurements at a greater depth, making the technique destructive and time consuming. This is specifically true of WC–Co coatings; moreover, electrolytic polishing of hard coatings like WC–Co is difficult.

## 2. Experimental methods

### 2.1. Rolling contact fatigue tests

A modified four-ball machine shown in Ahmed et al. [20] was used to examine the RCF performance of thermally sprayed rolling elements. This machine simulates the configuration of a deep groove rolling element ball bearing. It was used as an accelerated method for the evaluation of the RCF performance as many more stress cycles can be achieved in a fixed contact area. The coated rolling element cone was assembled to the drive shaft via a collet and drove the three planetary balls, which are free to rotate in a stationary cup. The drive coated cone represents the coated inner race and the three planetary balls act as the rolling elements in the configuration of the deep groove ball bearing. The stationary cup represents the outer race of a rolling element ball bearing in the contact model of the modified four-ball machine.

The cup assembly was loaded via a piston below the steel cup from a lever arm load to generate the required Hertz stress between the coated rolling element and the planetary balls. Conventional cleaning methods were used to avoid contamination of the contacting surfaces in the cup assembly before the RCF tests. The tests were conducted at an ambient temperature of approximately 24 °C. The spindle speed was set to $4000 \pm 5$ rpm using a high speed drive. The machine was set to stop when the vibration amplitude increased a preset maximum value due to the failure of any rolling element in the cup assembly. The cup assembly for the test configuration was of type II [21] having a surface hardness of 60 HRC. RCF tests were conducted in conventional steel ball bearing (steel plenary balls) and hybrid ceramic bearing (ceramic planetary balls) configurations. The steel lower balls were grade 10 (ISO 3290–1975) carbon chromium steel with an average surface roughness ($R_a$) of 0.02 μm and surface hardness of 64 HRC. The ceramic planetary balls were silicon nitride ceramic and manufactured by hot isostatically pressing. Ball blanks were ground and polished to a 12.7 mm diameter with an $R_a$ of 0.01 μm.

In order to access the performance of thermal spray coatings under various tribological conditions two lubricants were considered during the testing programme. Lubricant X was a high viscosity paraffin hydrocarbon which has a kinematic viscosity of 200 cst at 40 °C and 40 cst at 100 °C. This lubricant was not commercially available. Lubricant Y was a synthetic lubricant which has a kinematic viscosity of 12.5 cst at 40 °C and 3.2 cst at 100 °C. The RCF tests were conducted in immersed lubrication conditions. The RCF tests were conducted at the cup assembly loads of 40 N, 160 N, for the rolling element cones and 160 N, 400 N, 560 N for the rolling element balls. The ratio ($\lambda$) of the approximate value of the Elasto-Hydrodynamic Lubrication (EHL) film thickness [22] to the average surface roughness for the test lubricants X and Y under the given test conditions was calculated to be approximately $9 \pm 0.5$ and $1.5 \pm 0.25$ respectively for the given load. The exact values can be appreciated from Ahmed et al. [23,24].

#### 2.1.1. Coated ball rolling elements

A super D-Gun (SDG-2040) was used to deposit WC–Co coatings on the surface of 12.7 mm diameter rolling element balls. Only half of the ball was coated for the tests and the material composition of the coating can be summarised as: Co, 15%; C, 03%; and WC, 82%. The substrate material was sand blasted prior to the coating process and sprayed by several passes of spraying gun perpendicular to the direction of the wear track to obtain the as-sprayed coating thickness of 100 μm. The coated balls were ground and polished to attain an average coating thickness of approximately 60 μm. The average microhardness of the coating material was measured to be 1200 Hv (at 300p load), whereas the average substrate microhardness of the bearing steel substrate after thermal spraying was measured to be 600 Hv (at 100p load). The average surface roughness ($R_a$) of the coated rolling elements after polishing was measured to be 0.05 μm at a cutoff of 0.25 mm using a gaussian filter. The measurement direction for the average surface roughness was perpendicular to the rolling direction. Table 1 shows the RCF test results for the rolling element balls, in terms of the contact configuration, test lubricant and time to failure.

#### 2.1.2. Coated cone test elements

The drive cone test elements were thermally sprayed by HVOF process to form tungsten carbide cobalt (WC–12%Co) coatings on the surface of the mild steel cones having an apex angle of 109.2°. The substrate material was sand blasted and the rolling elements were coated in two different thickness by several passes of the spraying in a direction perpendicular to the cone axis. The rolling elements were ground and polished to give an average coating thickness of 150 μm and 50 μm. The average microhardness of the coating material was measured to be 1318 Hv (at 300p load), whereas the average substrate microhardness of the steel substrate after spraying was measured to be 218 Hv (at 300p load). The average surface roughness ($R_a$) of the coated rolling elements after polishing was measured to be 0.05 μm at a cutoff of 0.25 mm using a gaussian filter. The measurement direction for the average surface roughness was perpendicular to the rolling direction. Table 2 shows the RCF test results for the rolling element cones.

Table 1
RCF test results of D-Gun coated balls

| Test | Cup assembly load (N) | Planetary balls | Hertz contact stress [a] (GPa) | Lubricant | Time to failure (min) |
|---|---|---|---|---|---|
| A | 160 | Steel | 3.3 | X | 328 |
| B | 160 | Ceramic | 3.7 | X | 87 |
| C | 400 | Steel | 4.5 | X | 80 |
| D | 400 | Ceramic | 5.1 | X | 10 |
| E | 560 | Steel | 5.0 | X | 45 |
| F | 560 | Ceramic | 5.7 | X | 01 |
| G | 160 | Steel | 3.3 | Y | 10 |

[a] Uncoated contact conditions.

Table 2
RCF test results of HVOF coated cones

| Test | Cup assembly load (N) | Planetary balls | Hertz contact stress [a] (GPa) | Coating thickness (μm) | Time to failure (min) |
|---|---|---|---|---|---|
| H | 40 | Steel | 1.6 | 150 | 293 |
| I | 160 | Steel | 2.8 | 150 | 14 |
| J | 160 | Steel | 2.8 | 50 | 16 |

[a] Uncoated contact conditions.

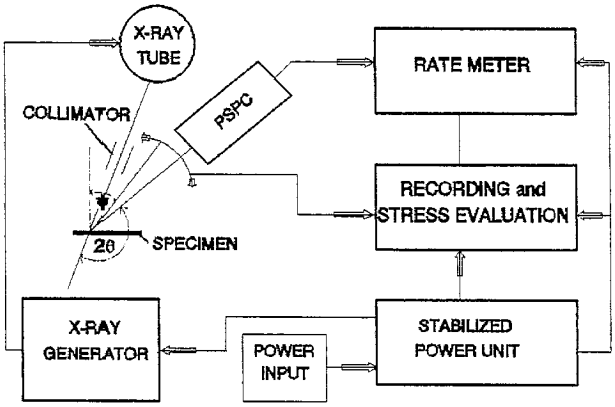


Fig. 2. Schematic diagram of residual stress measurement.

## 2.2. Residual stress measurements

Residual stress measurements using an X-ray diffraction, $\sin^2\psi$ technique, were performed on Rigaku RINT 2000 equipment. Fig. 2 is a schematic representation of the configuration used for the measurements. This equipment has a special residual stress attachment with a maximum capacity of 18 KW at 300 mA current and 60 kV voltage. The residual stress measurements, during this study, were performed at 40 kV voltage and 200 mA current. The X-ray diffraction results of residual stress in coatings were sensitive to the selection of the diffraction peak, elastic modulus, shape of the sample, time of measurement, surface roughness, and the orientation of the sample. The initial selection of the potential diffraction peaks for the residual stress measurements was made on the basis of the results of the X-ray diffraction pattern of the coating microstructure, using a wide angle goniometer. The diffraction results revealed the potential peaks for the residual stress measurements. Experimental analysis of the residual stress on the selected peaks led to the selection of the optimum peak, i.e. the peak which gives the most accurate statistical results at the maximum possible $2\theta$ angle. These tests revealed that a $2\theta$ angle of 125° for a Cr K$\alpha$ X-rays source gives maximum statistical confidence in the results. The selection of modulus of elasticity and Poisson's ratio values was made on the basis of previously obtained results using X-ray diffraction technique for an in-situ four-point bending test using the same equipment.

As the samples to be measured have the geometrical shapes of a ball and cone, the measurement areas were kept very small to minimize the effect of the curvature of the samples. This was done using small size collimators, i.e. 0.3 mm and 0.5 mm diameter. This requires a longer time for stress measurement. The results for other collimator sizes did not produce statistically confidant results. A position sensitive proportional counter (PSPC) of 24° and step angle 0.05° was used for the experimental analysis.

The orientation of the sample was found to have an influence on the stress results. For this purpose, an optical microscope was used to position the sample for each measurement. Considering the shape of the specimen and the anisotropy of the thermally sprayed coatings, residual stress measurements were made in three different directions. This enabled the investigation of the effect of measurement direction on the residual stress results. Finally, complex stress/strain relationships are used to predict the principal values of the stress. The stress measurement directions were 0°, 45° and, 90°. The coating anisotropy effect was minimised by performing the measurements parallel to the coating surface. An attempt was also made to measure the through thickness residual stress field of the coating cross-section but the diffraction profile was not significant for the residual stress measurements.

As the residual stress measurements were sensitive to the orientation of the specimen, a special technique was used to

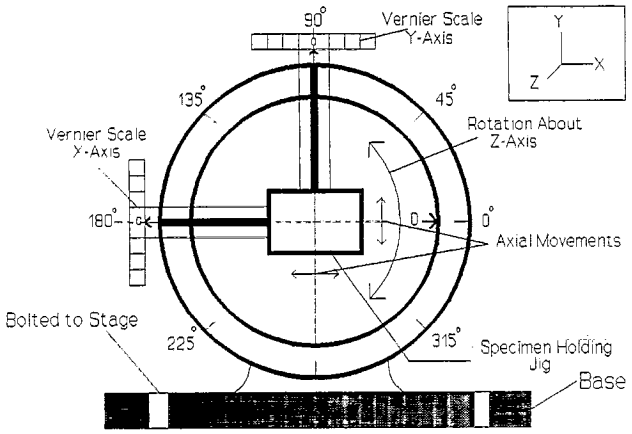


Fig. 3. Schematic diagram of sample rotation mechanism.

rotate the samples at the prescribed angle to change the orientation of the sample, while keeping the measurement point. For this purpose an arrangement shown in Fig. 3 was used. In this arrangement the sample had two axial motions, i.e. along the $x$ axis and $y$ axis, coupled with a rotational motion about the $z$ axis. The distance of sample from the collimator was kept constant by flushing the sample in a jig which was clamped at the centre of rotating mechanism. The first measurement was performed at 0° rotation, then the sample was rotated at 45° using the rotation about $z$ axis, while the measurement point was constantly kept at a reference point using optical microscope and $x$–$y$ axis motion of the sample for adjustments. The vernier divisions along the $x$ and $y$ axes gave an accurate measurement of 30 μm, while the degrees scale was marked at 0.1° for accurate rotation. The principal stress values and direction are then calculated using the standard relationships details of which can be seen in Warnock et al. [25].

## 3. Residual stress measurement results

### 3.1. Residual stress measurement results in D-gun coated balls

Fig. 4 represents the location and orientation of some typical residual stress measurements on D-Gun coated balls before and after the RCF tests. The numerical values of stress relating to these individual measurement points in three dif-

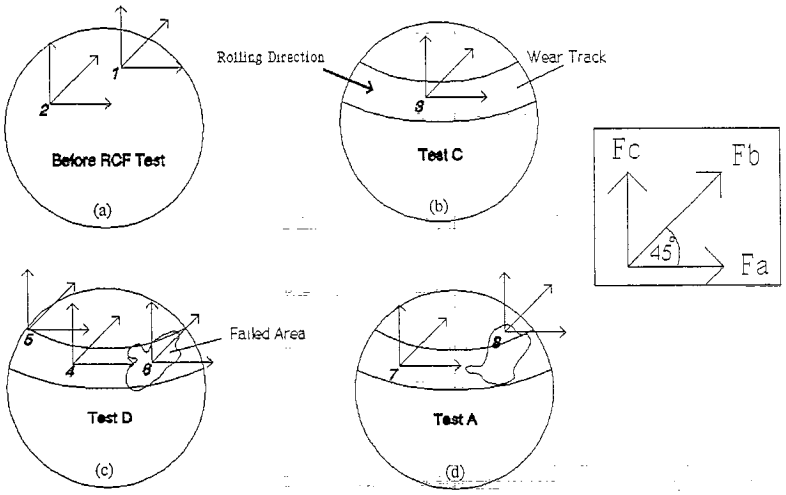


Fig. 4. Residual stress measurements on D-Gun coated balls.

Table 3
Residual stress results for D-Gun coated balls

| Measurement point | Test | Collimator size (mm) | Measurement time (min) | Residual stress values (MPa) | | | Principal stress (MPa) | | | Angle (°) |
|---|---|---|---|---|---|---|---|---|---|---|
| | | | | Fa (0°) | Fb (45°) | Fc (90°) | F1 | F2 | Max. shear | |
| 1 | Untested | 0.5 | 167 | −296±61 | −336±77 | −440±73 | −289 | −446 | +79 | +24 |
| 2 | Untested | 0.5 | 167 | −515±69 | −394±95 | −685±61 | −377 | −822 | +222 | +68 |
| 3 | C | 0.5 | 167 | −243±48 | −500±97 | −336±141 | −74 | −505 | +215 | −78 |
| 4 | D | 0.5 | 167 | −220±73 | [a] | −240±96 | [a] | [a] | [a] | [a] |
| 5 | E | 0.5 | 167 | −117±58 | −372±112 | −301±50 | −21.8 | −396 | +187 | −61 |
| 6 | D | 0.5 | 167 | −302±61 | [a] | −250±42 | [a] | [a] | [a] | [a] |
| 7 | A | 0.5 | 167 | −121±91 | [a] | −329±50 | [a] | [a] | [a] | [a] |
| 8 | A | 0.5 | 167 | −382±96 | [a] | −347±79 | [a] | [a] | [a] | [a] |

[a] Value not available.

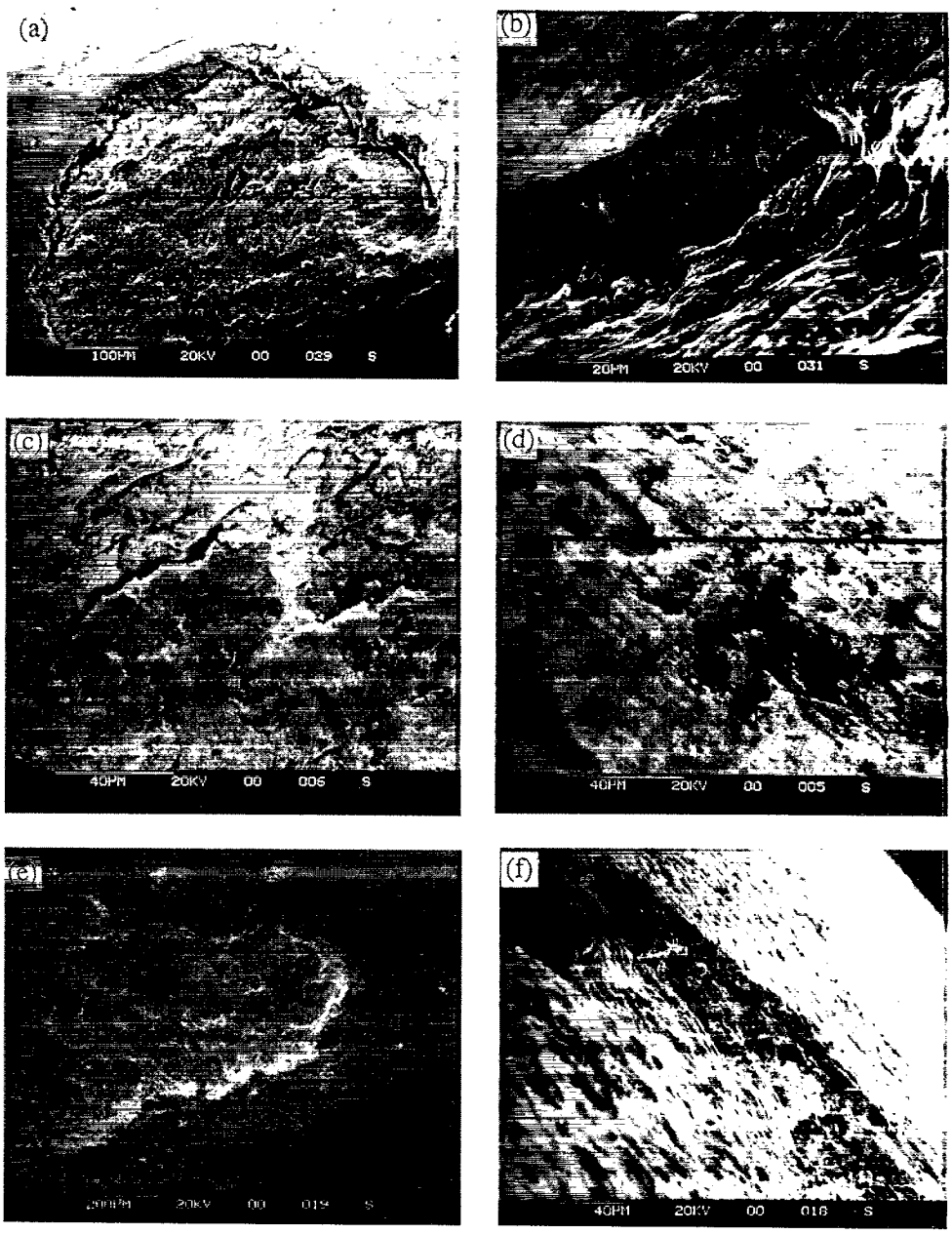


Fig. 5. SEM observations in D-Gun coated balls after RCF tests.

ferent directions can be appreciated from Table 3. The table also represents the principal stress values calculated from these measurements. The scanning electron microscopy (SEM) observations of the failed specimens used for the residual stress measurements can be appreciated from Fig. 5.

Fig. 4(a), represents the location of stress measurements before the RCF tests at two points, i.e. point 1, which is halfway between the wear track and crown of the ball while measurement point 2, is at a position on which the wear track will be formed during the RCF test. Fig. 4(b) represents the location of measurement point 3, which is in the middle of the wear track on a ball subjected to test C. Fig. 4(c), represents the location of three measurement points on the ball subjected to test D. The first set of measurements at point 4 are made in the middle of wear track, whereas point 5 represent the measurements at the edge of wear track. Measurement point 6 is located in the middle of the failed area within the wear track. The SEM observation at the residual stress measurement point in the failed area for the ball subjected to test D can be appreciated from Fig. 5(a), whereas Fig. 5(b) shows the cliff edge at a higher magnification. Fig. 5(c) shows the surface observation of the wear track after coating failure. Numerous cracks and loose debris particle can be seen after coating delamination. Fig. 5(d) shows the surface observation of the non delaminated section of the wear track for the test D. The figure shows the microcracks and deformations caused on the surface of the rolling elements during the RCF test. Fig. 4(d) represents the location of measurement points 7 and 8 on the ball subjected to test A. Point 7 is situated in the middle of the wear track, whereas point 8 is

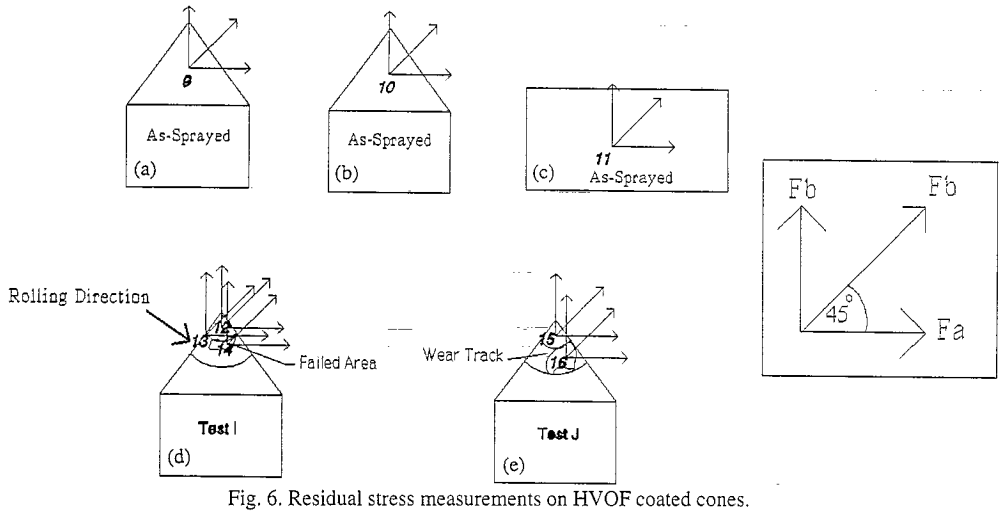


Fig. 6. Residual stress measurements on HVOF coated cones.

located at the edge of the wear track in the failed area. The SEM observations at the stress measurement point in the failed area for test A can be appreciated from Fig. 5(e), whereas Fig. 5(f) shows the cliff edge at a higher magnification. In some cases it is difficult to measure accurate diffraction peak shifts in the middle of the wear track, especially in the failed areas, mainly because of the poor surface roughness. The principal stress values for some of the measurement points in Table 3 are not included because of difficulty in measuring diffraction peak shifts.

### 3.2. Residual stress measurement results in HVOF coated cones

Fig. 6 represents the orientation and location of some measurements made on HVOF coated cones. The numerical values of stress relating to these individual measurement points in three different directions can be appreciated from Table 4. Fig. 6(a) represents the stress measurement point for a 200 μm thick coated cone in as-sprayed condition. Measurement point 9 is approximately at the location at which the wear track will be formed during the RCF test. Measurement point 10 in Fig. 6(b) represents the same for a 100 μm thick coated cone, whereas Fig. 6(c) represents the measurement point 11 on a flat plate in as-sprayed conditions.

Residual stress measurement point 12 on a cone subjected to test I can be appreciated from Fig. 6(d). This point is some distance from the wear track and located towards the cone apex, whereas measurement point 13 is at the edge of the wear track. Measurement point 14 is in the middle of the wear track within the failed area. Stress measurement points for the cone subjected to test J can be seen from Fig. 6(e). These measurements are made away from the wear track, and in the middle of the failed area.

Fig. 7 represents the SEM observations at the residual stress measurement points for RCF test I. Fig. 7(a) represents the overall view of the failed area, whereas Fig. 7(b) represents the failed area at a higher magnification. Fig. 7(c), represents the edge crack initiation, whereas Fig. 7(d) represents a higher magnification of the edge crack from a different orientation.

Fig. 8 represents typical residual stress measurement results for three orientations at measurement point 13. Fig. 8(a) represents the residual stress gradient obtained by the shift in diffraction peak. Fig. 8(b) and 8(c) represents the actual diffraction profiles for 0° orientation measurements at $\sin^2\psi$ value of 0.0 and 0.40 respectively.

Table 4
Residual stress results for HVOF coated elements (using Cr Kα source)

| Measurement point | Test | Collimator size (mm) | Measurement time (min) | Residual stress values (MPa) | | | Principal stress (MPa) | | | Angle (°) |
|---|---|---|---|---|---|---|---|---|---|---|
| | | | | Fa (0°) | Fb (45°) | Fc (90°) | F1 | F2 | Max. shear | |
| 9 | Sprayed | 0.3 | 167 | +75±38 | −72±110 | +232±44 | +392 | −85 | +238 | +71 |
| 10 | Sprayed | 0.5 | 167 | +12±31 | +62±24 | +127±50 | +127 | +12 | +58 | +7 |
| 11 | Sprayed | 1 | 33 | +148±62 | +37±56 | +148±62 | +259 | +37 | +111 | +90 |
| 12 | I | 0.5 | 133 | −216±35 | −244±30 | −246±28 | −211 | −250 | +20 | −41 |
| 13 | I | 0.5 | 133 | −436±33 | −308±50 | −369±20 | −302 | −502 | +100 | −70 |
| 14 | I | 0.5 | 167 | −43±21 | −52±4 | −453±94 | +35 | −531 | +283 | +44 |
| 15 | J | 0.3 | 133 | −237±41 | −385±48 | −288±33 | −137 | −387 | +125 | −78 |
| 16 | J | 0.3 | 167 | −123±90 | −101±89 | −151±82 | −98 | −175 | +39 | +3 |

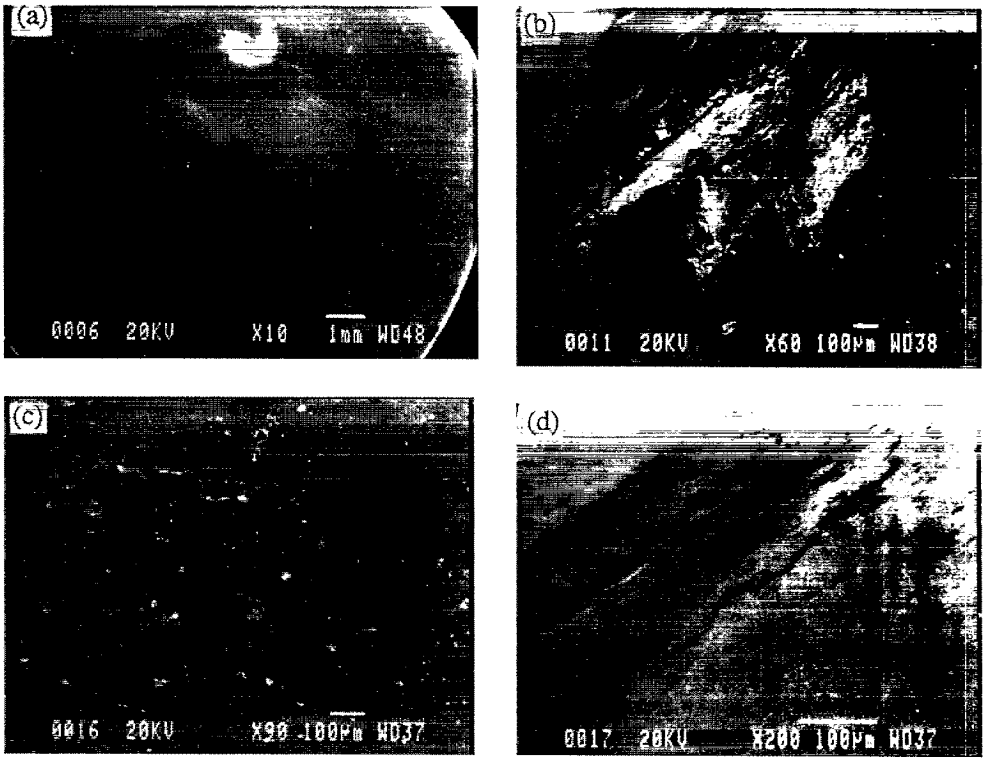


Fig. 7. SEM observations in HVOF coated cones after RCF tests I.

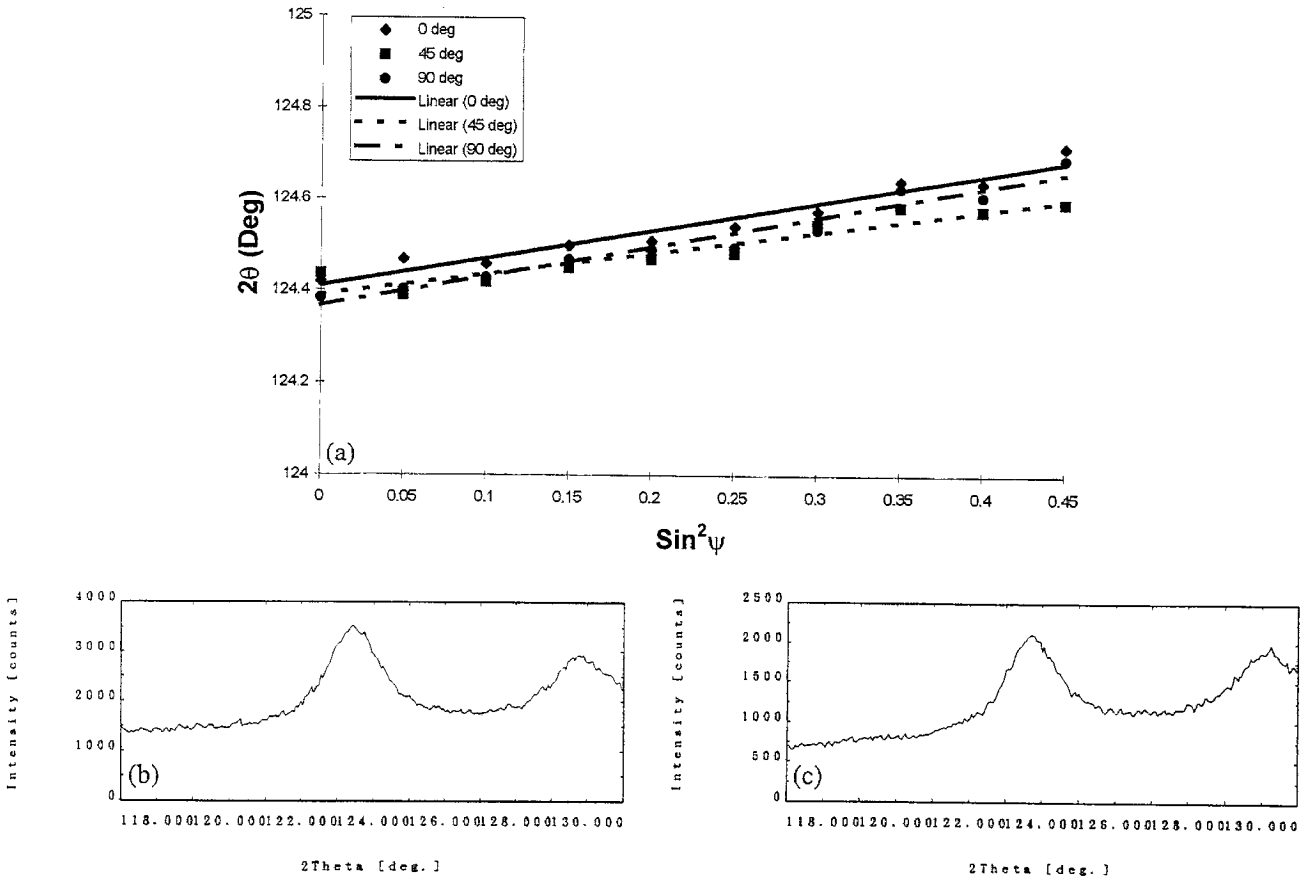


Fig. 8. Residual stress results at measurement point 13.

## 4. Discussion

Analyses of the first two residual stress measurement points on the surface of the pre-test rolling elements indicate the effect of the substrate geometry on the magnitude of the stress values. The area of the coated ball section at point 2 is greater than at point 1, and considering that the coating thickness is constant, higher stresses are generated at point 2 due to the substrate volume effects. A comparison of stress measurement results of the post-test rolling elements in the middle of the wear track, ie. measurement points 3, 4 and 7 which relates to the RCF tests C, D and A respectively, indicates that the magnitude of the compressive residual stress attenuate during the RCF test. This indicate that the nature of stress fields generated during the RCF tests was tensile in nature on the surface of the rolling elements. The magnitude of this stress change in the direction of rolling ranges from 300 to 400 MPa, calculated from the difference in stress values before and after the RCF test. It is appreciated that the depth of residual stress measurement is very near to the surface and stress changes are caused by the plastic flow and change in the contact area [26]. The surface changes are due to shakedown effects, microslip and asperity contact etc during the rolling contact. It should be appreciated that under steady state conditions plastic deformation due to shakedown can be present in a narrow layer near the surface [27] which can lead to residual stress generation. However, due to the lamella and brittle microstructure of thermal spray coatings microcracks appeared on the surface of the wear track (Figs. 5d, 7c and 7d) during the rolling contact which attenuated the residual stress on the surface of the rolling elements. This effect was more prominent on the failed coating areas (Fig. 5c) where the coating microstructure fractured leading to loose debris particles. The fact that the depth of residual stress was limited to a few microns indicate that the cyclic plastic strain in this near surface layer relaxed the stresses during the rolling contact. However, the studies relating to the plastic deformation of the coating microstructure within the wear track requires transmission electron microscopy (TEM) analysis. This analysis was not carried out during this work. The subsurface residual stress fields can thus be different from surface stress values as indicated in the studies by Muro et al. [5]. Hence, the effect of the residual stress changes caused by the shakedown phenomenon in thermally sprayed surfaces is not clear at this stage. However, the analytical approaches to measure the shakedown effects in coated elements [29], indicate that it is possible to calculate the shakedown effects for coated elements (in sliding contact) and the shakedown can improve the performance if the coating thickness is greater is than a critical value (depending upon the elastic and the plastic properties), unfortunately thermal spray coatings are neither homogenous nor isotropic which makes the shakedown analysis complicated in rolling contact. An experimental approach by measuring the surface and subsurface residual stress fields can thus provide an understanding of the residual stress fields in thermal spray coatings due to rolling contact. The magnitude of the residual stress generation during the RCF tests depends upon the test duration and the magnitude of the Hertz contact stress during the test. However, it is difficult to appreciate that which of the two factors has the more significant effect on the residual stress. The residual stress measurements also indicate that the measurements perpendicular to the direction of rolling show less change in surface stress values after the rolling contact. There are two main reasons postulated for this difference in the magnitude of stress generation in the two directions, i.e. along the rolling direction and a direction perpendicular to it. Firstly, the rolling motion causes a maximum variation in the stress value at the leading and trailing edge of the contact along the direction of rolling, i.e. the stress range is maximum along the direction of rolling. Secondly, the Hertz contact stress (compressive) value is maximum in the middle of wear track and minimum at the edge of the contact area (tensile) which affects the residual stress generation. It is appreciated that the polishing of samples before RCF tests could have caused some changes in the residual stress values. Hence the calculations for the residual stress generation due to RCF testing are performed on the basis of the difference in the stress values for the polished samples and the values after RCF tests. This is done to ensure that the stresses are representative of RCF testing only and these stresses indicate the residual stress fields in thermal spray coatings which have high compressive residual stress due to the spraying process.

A comparison of stress measurement results of as-sprayed samples, i.e. measurement points 9, 10, and 11, indicates that the stress values are dependent upon the geometry of the sample and the coating thickness. This is in accordance with the work reported by Brandt [14]. Stress measurement results indicate that for the coating on a flat substrate the stress values do not change in axial and longitudinal directions. This can be appreciated from the residual stress values for a flat plate at measurement point 11, which are exactly the same at 0° and 90°. However, for conical shaped specimens these values change in the three directions of measurement for the two coating thicknesses. This is mainly because the rate of heat transfer varies along the axis of the cone, i.e. from the apex to the base of the cone. It is important to appreciate that the coefficient of thermal expansion (CTE) of the steel substrate is approximately twice that of the WC–Co coating. This should result in a net compressive stress in the coating. However the as-spared samples show residual stress of tensile nature. This is mainly a result of the following two factors.

(a) Firstly, the depth of measurement by X-ray diffraction technique for most of the coatings is limited to a few microns [28], which represents the coating deposited in the final pass of thermal spraying process. The quenching stresses will thus be significant at this depth, moreover there will be no shot-peening effect on the final layer of coating.

(b) Secondly, the affect of residual stress caused by the difference in CTE of the coating and the substrate is more significant near the interface. The intensity of stress due to this effect will reduce with the increase in distance from the

interface. This can also be the reason for slightly higher tensile residual stress values for 200 μm thick coatings in comparison to a 100 μm thick coating. This behaviour is evident by the analysis performed by Greving et al. [28], Gudge et al. [29], Knight et al. [12] and Provot et al. [10], in which the residual stress values change from tension to compression within the coating thickness.

An analyses of residual stress measurements in the middle of fractured coatings (some of which are shown in Figs. 4 and 6), e.g. measurement points 14 and 16, shows very low compressive stress values at the depth of failure with the exception of measurement point 6. This indicates that the crack propagation relaxed the compressive residual stresses generated by thermal spraying process. Moreover, it is also possible that the crack propagation was in Mode I (tensile). However, several other factors, e.g. brittle or ductile fracture, subsurface plastic strain, interlamella cracking due to applied stress leading to micro and micro stress relaxation [30] etc. can also have an effect. The SEM analyses of the failed specimens reveal that these coatings do not fail near the interface, which is mainly because of high compressive residual stresses [1] near the interface and the mechanical interlock caused by the sandblasting of substrate. Moreover, the depth of failure in the coated specimens was shown by the author [23] to correspond to orthogonal shear stress. It is interesting to note that several cracks can be seen within the coating microstructure above the depth of failure (Fig. 5(a) and (b)) but coatings do not delaminate at these depths, which represent that under the given tribological conditions the failure was subsurface crack propagation at different depths.

In general, residual stress measurement results presented in Tables 3 and 4 show variation in the stress values, not only in the as-sprayed samples of different geometries, but also after the RCF tests. Principal residual stress analysis indicate that the magnitude of maximum shear stress generated during rolling contact can be several hundred of MPa which can be crucial for the RCF performance. Moreover, the residual stress measurements for the D-Gun and HVOF coated elements after the RCF test attenuate the effect of stresses induced by the spraying process due to plastic deformation caused by a load exceeding the elastic limit.

## 5. Conclusions

1. The magnitude of compressive residual stress due to the spraying process attenuates during the RCF test which can be due to the deformation and microcracking during the rolling contact. The residual stress attenuation is higher in the near-surface layer of the wear track in the direction of rolling.
2. The failed coating areas show low compressive residual stress indicating high relaxation of compressive residual stress during the coating fracture.
3. The residual stress values in the rolling elements change with the direction of stress measurement and with the change in substrate geometry.

## 6. Abbreviations

| | |
|---|---|
| APS | air plasma spraying |
| CDS | continuous detonation gun |
| CTE | coefficient of thermal expansion |
| D-Gun | detonation gun |
| $E$ | elasticity modulus |
| $F_1$ | maximum principal stress |
| $F_2$ | minimum principal stress |
| $F_a$ | residual stress measurement at 0° rotation |
| $F_b$ | residual stress measurement at 45° rotation |
| $F_c$ | residual stress measurement at 90° rotation |
| HVOF | high velocity oxy-fuel |
| PSPC | position sensitive proportional counter |
| $R_a$ | average surface roughness |
| RCF | rolling contact fatigue |
| SEM | scanning electron microscopy |
| WC–Co | tungsten carbide cobalt coating |
| $\nu$ | Poisson's ratio |
| $\mu$ | micron |
| $\theta$ | diffraction angle |
| $\theta_0$ | principal direction with respect to 0° measurement ($F_a$) |
| $\theta_d$ | diffraction angle in a stress-free condition |
| $\psi$ | angle between the sample normal and diffraction plane normal |

## Acknowledgements

The authors of this paper would like to acknowledge Professor Shogo Tobe of Ashikaga Institute of Technology, Japan, for his help in the preparation and stress measurement of coatings. Authors also acknowledge the support by the Overseas Research Scholarship Scheme which is partly funding this research project.

## References

[1] J.C. Clark, Fracture tough bearings for high stress applications, *Proc. 21st Joint Propulsion Conference*, 1985, Paper AIAA-85-1138.
[2] J.J. Bush, W.L. Grube and G.H. Robinson, Microstructural and residual stress changes in hardened steel due to rolling contact, *Rolling Contact Phenom.*, (1962) 365–399.
[3] E.V. Zaretsky, R.J. Parker and W.J. Anderson, A study of residual stress induced during rolling contact, *Trans ASME J. Lubrication Technol., 91F* (1969) 314–319.
[4] R.J. Pomeroy and K.L. Johnson, Residual stresses in rolling contact, *J. Strain Anal., 4* (3) (1969) 208–218.
[5] H. Muro, N. Tsushima and K. Nunome, Failure analysis of rolling bearings by X-ray measurement of residual stress, *Wear, 25* (1973) 345–356.

[6] Q. Chen, G.T. Hahn, C.A. Rubin and V. Bhargava, The influence of residual stresses in rolling contact mode II driving force in bearing raceways, *Wear, 126* (1988) 17–30.

[7] S. Kuroda, T. Fukushima and S. Kitahara, Significance of the quenching stress in the cohesion and adhesion of thermally sprayed coatings, *Conf. Proc. Int. Thermal Spray Conference, Orlando, FL,* ASM International, Ohio, 44073, USA, 1992, pp. 903–909.

[8] S.C. Gill, Residual stress in plasma sprayed deposites, Ph.D. Thesis, Conville and Cains College, Cambridge, UK, 1993.

[9] .S.K. Wong and A. Kapoor, The effect of hard and stiff overlay coatings on the strength of surfaces in repeated sliding. Tribol. Int. Vol. 29, No. 8 (1996) 698-702.

[10] X. Provot, H. Burlet, M. Vardavoulias, M. Jeandin, C. Richaed, J. Lu and D. Manesse, Comparative studies of microstructures, residual stress distribution and wear properties for HVOF and APS WC–Co coatings of Ti6Al4V, *Conf. Proc. National Thermal Spray Conference, Anaheim, CA,* ASM International Ohio, 44073, USA,1993, pp. 159–166.

[11] D.J. Greving, E.F. Rybicki and J.R. Shadley, Through-thickness residual stress evaluations for several industrial thermal spray coatings using a modified layer removal method, *J. Thermal Spraying, 3* (1994) 379–388.

[12] R. Knight and R.W. Smith, Residual stress in thermally sprayed coatings, *Conf. Proc. National Thermal Spray Conference, Anaheim, CA,* ASM International, Ohio, 44073, USA, 1993, pp. 607–612.

[13] T. Morishita, E. Kuramochi, R.W. Whitfield and S. Tanabe, Coatings with compressive stress, *Conf. Proc. Int. Thermal Spray Conference, Orlando, FL,* ASM International, Ohio, 44073, USA, 1992, pp. 1001–1004.

[14] O.C. Brandt, Mechanical properties of HVOF coatings, *J. Thermal Spraying, 4* (1995) 147–152.

[15] H. Nakahira, K. Tani, K. Miyajima and Y. Harada, Anisotropy of thermally sprayed coatings, *Conf. Proc. Int. Thermal Spray Conference, Orlando, FL,* ASM International, Ohio, 44073, USA, 1992, pp. 1011–1017.

[16] R. Kawase and K. Tanaka, Study on elastic constant and residual stress measurements during ceramic coatings, *Conf. Proc. National Thermal Spray Conference, Long Beach, CA,* ASM International, Ohio, 44073, USA, 1990, pp. 339–342.

[17] G.H. Farrahi, P.H. Markho and G. Maeder, A study of fretting wear with particular reference to measurement of residual stress by X-ray diffraction, *Wear, 148* (1991) 249–260.

[18] B.D. Cullity, *Elements of X-ray Diffraction*, Addison–Wesley, Reading, MA, 1978.

[19] M. Hadfield, T.A. Stolarski and R.T. Cundill, Failure mode of ceramics in rolling contact, *Proc. R. Soc Lond. A, 443* (1993) 607–621.

[20] R. Ahmed and M. Hadfield, Rolling contact fatigue performance of detonation gun coated elements, *Tribol. Int., 30* (2) (1997) 129–137.

[21] V. Kruger and W.J. Bartz, Comparison of different ball fatigue test machines and significance of test results to gear lubrication, *Rolling Contact Fatigue Performance Testing of Lubricants,* Inst. of Petroleum, UK, 1977, pp. 137–159.

[22] B.O. Jacobson, *Rheology and Elastohydrodynamic Lubrication*, Baker and Taylor, Elsevier, Netherlands, 1991.

[23] R. Ahmed and M. Hadfield, Rolling contact fatigue behaviour of thermally sprayed rolling elements, *Surf. Coatings Technol., 82* (1996) 176–186.

[24] R. Ahmed and M. Hadfield, Rolling contact fatigue performance of HVOF coated elements, *Conf. Proc. 4th Int. Conf. on Advances in Surface Engineering, Newcastle upon Tyne, UK, The Royal Society of Chemistry, UK 1997,* in press.

[25] F.V. Warnock and P.P. Benham, *Mechanics of Solids and Strength of Materials*, Pitman Press, Bath, 1965.

[26] A. Kapoor and K.L. Johnson, Effect of changes in contact geometry on shakedown of surfaces in rolling/sliding contact, *Int. J. Mech. Sci., 34* (3) (1991) 223–239.

[27] K.L. Johnson, *Contact Mechanics*, Cambridge University Press, Cambridge, UK, 1985.

[28] D.J. Greving, J.R. Shadley and E.F. Rybicki, Effects of coating thickness and residual stresses on the bond strength of ASTM C633-79 thermal spray coating test specimens, *J. Thermal Spraying, 3* (1994) 371–378.

[29] M. Gudge, D.S. Rickerby, R. Kingswell and K.T. Scott, Residual stress in plasma metallic and ceramic coatings, *Conf. Proc. National Thermal Spray Conference, Long Beach, CA,* ASM International, Ohio, 44073, USA, 1990, pp. 331–337.

[30] C.K. Lin, S.H. Leigh and C.C. Brendt, Investigation of plasma sprayed materials by vickers indentation tests, *Conf. Proc. Int. Thermal Spray Conference, Kobe, Japan,* High Temperature Society of Japan, 1995, pp. 903–908.